Hindawi
Advances in Materials Science and Engineering
Volume 2023, Article ID 1366857, 9 pages
https://doi.org/10.1155/2023/1366857

Research Article

Optimization of Process Parameters in Electrochemical Micromachining of AMCs by Using Different Techniques of Weight Evaluation

S. Maniraj,[1] **R. Thanigaivelan**,[2] **K. Gunasekaran**,[3] **and K. G. Saravanan**[4]

[1]*Department of Mechanical Engineering, Paavai Engineering College (Autonomous), Namakkal, Tamilnadu, India*
[2]*Department of Mechanical Engineering, AKT Memorial College of Engineering and Technology, Kallakurichi, Tamilnadu, India*
[3]*Department of Mechanical Engineering, Muthayammal Engineering College (Autonmous), Rasipuram, Tamilnadu, India*
[4]*Department of Mechanical Engineering, Sona College of Technology, Salem, Tamilnadu, India*

Correspondence should be addressed to R. Thanigaivelan; tvelan10@gmail.com

Received 28 April 2022; Revised 3 September 2022; Accepted 30 September 2022; Published 22 February 2023

Academic Editor: Abílio De Jesus

The application of electrode heating is proposed in electrochemical micromachining (EMM). In the EMM process, the temperature of the electrode, voltage, duty cycle, and electrolyte concentration are considered process parameters. Taguchi L_{18} mixed-level orthogonal array (OA) design was adopted for designing the experiments and this study highlights the effect of temperature on responses such as radial overcut (ROC), material removal rate (MRR), and conicity factor (CF). In addition, multicriterion design making (MCDM) with VIKOR (VlseKriterijumska Optimizacija I Kompromisno Resenje, i.e., multi-criteria optimization and compromise solution) technique is used for finding the best alternatives based on the distinct weight assessing methods such as equal weights method (EWM), analytic hierarchy process (AHP), and entropy-based weights method (EBWM). Furthermore, a confirmation test is also conducted to find the best optimal parameters and their levels among the EWM-VIKOR, AHP-VIKOR, and EBWM-VIKOR. The results revealed that AHP-VIKOR provides a maximum improvement of 0.945 among the three methods.

1. Introduction

Composite materials nowadays play a vital role in engineering applications such as automotive, aerospace, and other industrial areas. In particular, MMCs with high specific stiffness and high strength may be used in long-term applications where weight reduction is a key factor, such as robots, turbine blades, high-speed machinery, rotating shafts, and automotive engine and brake components. However, the machining of composite materials is still difficult in the conventional machining process due to the reinforcement present in matrix material [1, 2]. Nonconventional machining processes are commonly utilized regardless of material hardness. In particular, microfabrications of composites are machined through processes such as electrochemical micromachining (EMM), electrical discharge machining (EDM), laser beam machining (LBM), and chemical machining (CM). Among these machining processes, EMM plays a major role due to better surface finish, higher machining rate, and high precision to be achieved. EMM process works on the reverse electroplating process under Faraday's law [3–5]. In this proposed work, the temperature of the electrode is considered one of the parameters for all the experiments run. In electrochemistry, temperature is the most influencing factor in improving the movement of ions between the electrodes. Researchers have performed experiments in EMM with different methods of heating such as ultraviolet light, infrared light source, ultrasonic vibration heating, and coil heating for improving the machining efficiency [6, 7]. Gründler et al. utilized an AC power supply for heating the electrode rather than supplying DC in the perspective of

reducing the faradic impacts that contribute to more electrons being transferred between the electrodes [8]. Qiu et al. implemented a new technique of radiofrequency (Rf) radiation heating the electrode. The heated electrode changes the viscosity property of the electrolyte solution resulting in enhanced flow patterns that contribute to enhanced mass transportation [9]. Wildgoose et al. examined the changed heating strategies in electrochemistry and discussed high-temperature mass transport. During the production of greater current, the phenomenon of mass transport increases through convection [10]. Frank Marken used microwave irradiation to identify a novel approach for heating nonisothermal electrodes. They noted a greater energy supply at high temperatures through this heating principle [11]. Long et al. suggested laser support for the electrochemical processing of stainless steel material. The electrolyte temperature variation creates greater conductivity resulting in a greater material dissolution rate [12].

Any manufacturing process is required to meet the quality and cost. The optimization of process parameters improves productivity and cost. Researchers have used MCDM to optimize the responses. Maniraj et al. adopted the Taguchi technique for optimizing the MRR and ROC by considering different % compositions of GGBS. In addition, the MCDM method of TOPSIS is also utilized for finding the best solution [13]. Singaravel et al. combined the AHP and TOPSIS for maximizing the MRR and minimizing the surface roughness (SR) and microhardness in the turning operation. The AHP method is used for finding the weight factor based on the decision makers and it provides a better solution when compared to other alternatives [14]. Kumar et al. also considered multicriterion optimization by assessing the weight by different methods such as equal weight method (EWM), AHP, and entropy-based weight method (EBWM) for consumption of energy responses along with MRR and SR during the turning operation [15]. Dinesh Singh et al. evaluated the performance of ECM process parameters by using the black hole algorithm (BHA) and the result obtained by using BHA provides better results when compared to other algorithms [16]. Sohrabpoor et al. designed a combined MCDM method of principal component analysis (PCA) with neuro-fuzzy associated with the teaching cuckoo algorithm for finding the optimal parametric condition satisfying maximum MRR, minimum ROC, and SR [17]. Bhuyan et al. optimized the process parameters of the EDM process by using an entropy-based assigning weight with the VIKOR method. Additionally, a confirmation test to validate optimized outcomes is also performed [18]. Maniraj et al. utilized a novel approach for heating the electrode through an AC power supply and corresponding effects were studied based on the temperature of aluminium metal matrix composite (AMC) with 12% reinforced GGBS material [19].

Based on the above literature, the researchers use electrode heating in the field of electrochemistry, but still, researchers are not focused on electrode heating in the EMM process. The heating of the electrode tool is suggested in this research study and an appropriate heating system for heating the cathode device to the given temperature and maintaining the electrode temperature with the aid of a thermostat sensor. In addition, the MCDM optimization technique (VIKOR method) was used to maximize the MRR, minimizing the ROC and CF. In this work, three distinct techniques (EWM, AHP, and EBWM) are used for assessing the weights because these methods have different principles for finding the weights. Furthermore, a confirmation test is also conducted for obtaining optimum parametric conditions by using the VIKOR index and then reported in this study.

2. Experimental Setup and Experimentation

Figure 1 shows the modified experimental setup for conducting the designed work. It consists of a feeding system, a machining unit, a system for supplying the electrolyte, a power supply unit, and a newly designed heating electrode unit. This heating unit is made up of a heating coil, thermostat, regulator unit, power supply unit, and ceramic material. As shown in Figure 2, the heating unit is placed on the electrode tool. In experimentation, the temperature of the electrode tool is set using the regulator for controlling the temperature and then it is heated by using the supply of AC power. Here, the ceramic material is used to prevent the conduction of the AC power supply between the heating coil to the tool electrode. The thermostat is provided in the system for continuous monitoring of temperature and maintains the set electrode tool temperature. If the temperature of the electrode instrument reaches the set temperature, the thermostat breaks the AC power supply automatically to the coil responsible for heating the electrodes. The temperature range varies between 20°C to 60°C.

Al 6061 T6 material is used as a matrix and 12% composition of GGBS by weight is used as reinforcement for fabricating the AMCs in the stir casting technique [20]. Selected matrix material and reinforcement chemical composition are presented in Tables 1 and 2.

The temperature of the electrode, electrolyte concentration, duty cycle, and machining voltage is selected as machining parameters and it is presented in Table 3 with their levels. The different levels of these parameters are selected based on the set of preliminary experiments. In this process, the current and frequencies are kept constant.

The output parameters such as MRR, ROC, and CF evaluate the performance of the EMM process. MRR is determined by the difference in the period of time between the work piece's final and initial weights. The duration of the machining process is calculated for all the experiments for computing the MRR. ROC is computed from the difference between the diameters of the tool electrode to the diameter of the machined hole. CF is deliberated by the expression which is $\mathrm{CF} = (T_d - B_d)/2 * w$, where T_d is the top hole diameter, B_d is the bottom hole diameter, and "w" is the workpiece thickness [21]. Machined hole diameters are identified through the scanning electron microscope (SEM) and it is used to figure out the ROC and CF. L_{18} mixed-level OA is used to design the experiments and it is presented in

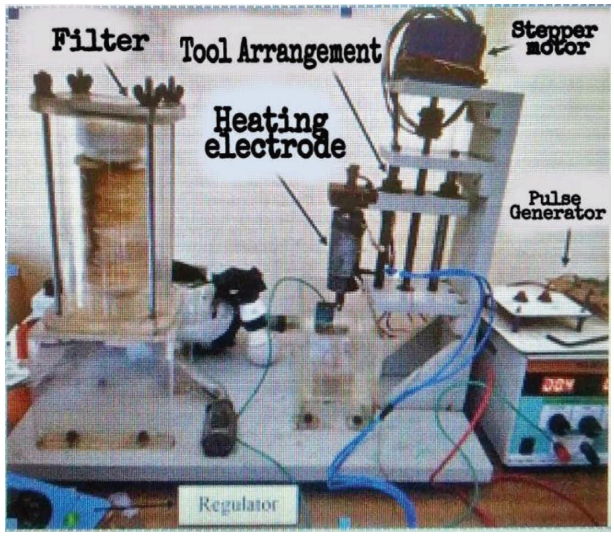

Figure 1: Modified EMM setup used for experimentation.

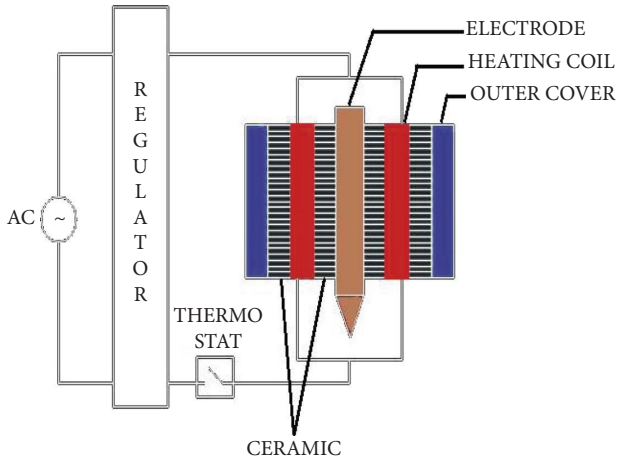

Figure 2: Designed heating unit for EMM process.

Table 4. Higher MRRs reduced ROCs and reduced CFs are preferred in the EMM process.

3. Results and Discussion

Figure 3 illustrates the 3-Dimensional response surface plot of MRR varying with the temperature of the electrode, voltage, duty cycle, and electrolyte concentrations. Figure 3(a) depicts the increase in temperature of the electrode leads to an increase of MRR due to the microstirring effect which is produced because of its temperature changes, irrespective of its voltage [22]. The current density needed for machining the AMCs rises with an increase in the duty cycle, simultaneously contributing to the linear increase of MRR for the heated electrode. The temperature of the electrode and higher current density dissolve the matrix material and at the same time break the reinforcement bond leading to greater MRR and it is evident from Figures 3(b). From Figure 3(c) it's evident that MRR increases with sodium nitrate electrolyte concentration. The precipitation and sludge formations are reduced due to the combined effect of the microstirring effect and proper flushing of electrolytes which leads to an increase in the MRR [23]. Figure 4 illustrates the 3-dimensional response surface plot of ROC varied with voltage, duty cycle, and electrolyte concentration comparatively with the temperature of the electrode. In electrochemistry, the movement of ions in an electrolyte solution is directly proportional to the temperature which contributes to increased conductivity. In AMCs, the distribution of reinforcement also plays a vital role because ceramic reinforcement has lesser conductivity when compared to matrix material [24].

Due to the distinct thermal expansion coefficients, the separation of reinforcement material (GGBS) from the

Table 1: Aluminium 6061 T6 quantified chemical composition in %.

Materials	Si	Cu	Fe	Mg	Cr	Mn	Zn	Ti	Al
Percent	0.80	0.40	0.70	1.2	0.35	0.15	0.25	0.15	Balance

Table 2: GGBS constituents' chemical composition quantified in %.

Materials	SiO_2	CaO	Al_2O_3	MgO	SO_3	K_2O	Na_2O	Fe_2O_3
Percent	34.4	33.2	21.5	9.5	0.47	0.39	0.34	0.2

Table 3: Parameters of machining and their levels.

Symbol	Parameters	Levels		
		1	2	3
A	Temperature of the electrode (°C)	30	40	—
B	Machining voltage(V)	8	10	12
C	Duty cycle (%)	70	80	90
D	Electrolyte concentration (g/lit)	15	20	25

Table 4: L_{18} mixed-level OA-based experimental design.

Experimental no.	A	B	C	D	MRR (gm/min)	ROC(μm)	CF
1	30	8	70	15	0.071	46	0.023
2	30	8	80	20	0.073	57	0.021
3	30	8	90	25	0.074	78	0.018
4	30	10	70	15	0.075	53	0.017
5	30	10	80	20	0.078	68	0.015
6	30	10	90	25	0.080	92	0.013
7	30	12	70	20	0.086	78	0.010
8	30	12	80	25	0.088	94	0.010
9	30	12	90	15	0.081	74	0.009
10	40	8	70	25	0.094	103	0.026
11	40	8	80	15	0.091	82	0.023
12	40	8	90	20	0.093	88	0.024
13	40	10	70	20	0.096	98	0.021
14	40	10	80	25	0.098	112	0.015
15	40	10	90	15	0.093	81	0.016
16	40	12	70	25	0.114	110	0.019
17	40	12	80	15	0.091	96	0.017
18	40	12	90	20	0.094	102	0.016

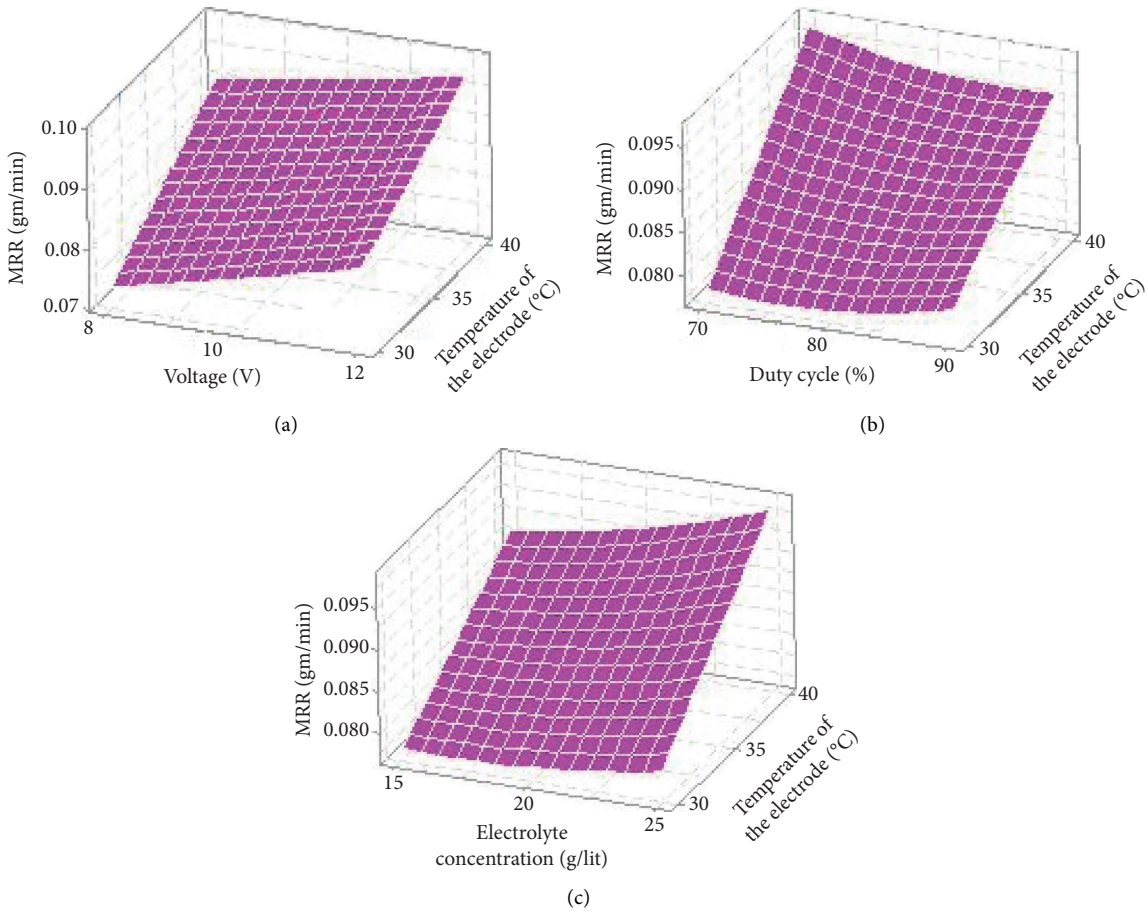

Figure 3: Process parameters effect on MRR.

AMCs also increases with increased the temperature of the electrode. This attribute leads to higher ROC from AMCs and it is evident in Figures 4(a) and 4(b). From Figure 4(c), with the increased concentration of electrolytes, the associated machining ions are also increased. This increase in ion and electrode heating removes more materials in the machining area, including the required material, resulting in higher ROC [25].

Figure 5 illustrates the 3-dimensional response surface plot of CF varied with voltage, duty cycle, and electrolyte concentration comparatively with the temperature of the electrode. The impact of electrode temperature on CF is shown in Figure 5(a). Electrode heating establishes the hot spot/zone in front of the electrode. Gas bubbles form at the electrode attributing to increasing the electrolyte conductivity thereby it reduces the CF when increase in voltage.

Because of the distribution of the reinforcement in the MMC, the removal of bulk material from the microstirring impact leads to an increase in CF during longer pulse duration and it is evident from Figure 5(b). It is clear from Figure 5(c), the temperature of the electrode initiates quicker ion movement and the microstirring impact also dissolves the dissolved products. This impact, resulting in less conicity when compared with increases in the concentration of the electrolyte, replenishes the electrolyte in the machining area [6].

3.1. Integrated MCDM Method with EWM, AHP, and EBWM-VIKOR Approach. In this research work, an integrated MCDM method was adopted. It consists of various weights assessing methods such as EWM, AHP, and EBWM with the VIKOR method [15]. The steps to be followed for implementing the MCDM technique are as follows:

Step 1. Decision Matrix Development

In optimization techniques, the development of a decision matrix is important with considering the alternatives as input/process parameters and the criteria as output parameters. The formulation of the decision matrix by using the expression provided in the following equation:

$$\mathrm{DM}_{ij} = \begin{bmatrix} & C_1 & C_2 & \ldots & C_n \\ A_1 & a_{11} & a_{12} & \ldots & a_{1n} \\ A_2 & a_{21} & a_{22} & .... & a_{2n} \\ \ldots & \ldots & .... & .... & .... \\ A_m & a_{m1} & a_{m2} & .... & a_{mn} \end{bmatrix}, \quad (1)$$

where $i = 1, 2, 3, \ldots, m$ represents the number of possible alternatives present, and $j = 1, 2, 3, \ldots, n$ represents the number of individual criteria.

Step 2. Determination of Normalized Decision Matrix

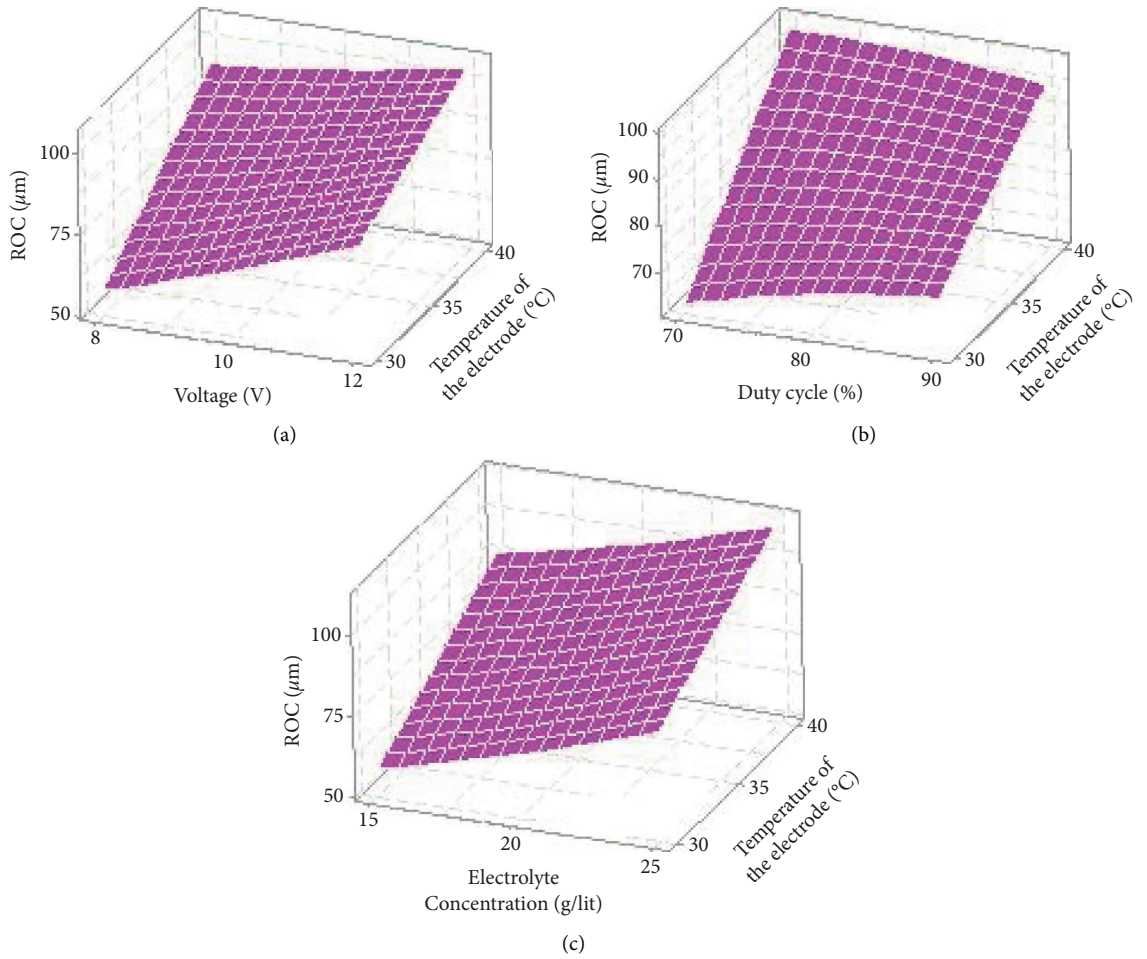

Figure 4: Process parameters effect on ROC.

In this step, all the criteria/output parameters are normalized irrespective of their unit and convert the values of the criteria lie between 0 and 1 by using the following equation:

$$NDM_{ij} = \frac{a_{ij}}{\sum_{i=1}^{m}\left(a_{ij}\right)^2}; \quad i = 1, 2, 3, m; \; j = 1, 2, 3, n; . \tag{2}$$

Step 3. Determination of Weights of Different Criteria/Output Parameters

In this particular step, identifying and assigning the different weights W_j (for $j = 1, 2, 3, \ldots, n$) by using the different weight assessing methods such EWM, AHP, and EBWM.

3.1.1. Equal Weight Method. In this EWM, the weights of individual criteria are considered by dividing 1 by the number of individual criteria (n) as expressed in the following equation:

$$Wj = (\text{for}\, j = 1, 2, n) = \frac{1}{n}. \tag{3}$$

In this research work, there are three (3) criteria are considered, so the weight of individual criteria is calculated by the following expression as shown in the following equation:

$$Wj(\text{for}\, j = 1, 2n) = \frac{1}{3}. \tag{4}$$

Based on EWM, the respective weights of MRR, ROC, and CF are 0.33, 0.33, and 0.33, respectively.

3.1.2. Analytic Hierarchy Process. The AHP method requires decision makers to make decisions as to the comparative significance of each criterion and then indicate a preference for each alternative decision on each criterion [25].

Based on AHP, the respective weights of MRR, ROC, and CF are 0.63, 0.26, and 0.11, respectively.

3.1.3. Entropy-Based Weights Method. In this EBWM, the weights of the individual criterion are measured without the influence of the decision maker. Based on the decision matrix as expressed in (1), normalization of the matrix with minimization and maximization criterion is formulated. Criterion weights are critical in measuring the performance

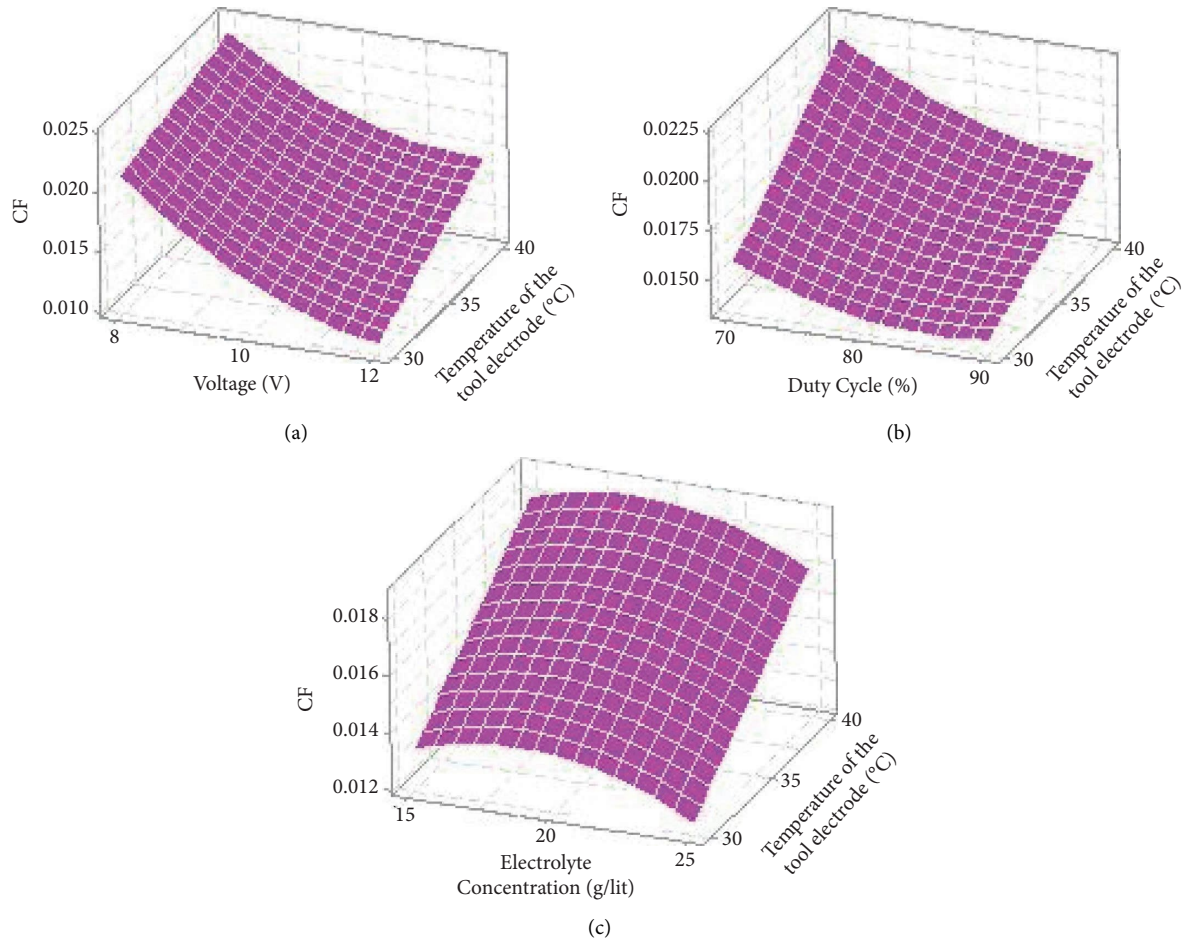

Figure 5: Process parameters effect on CF.

Table 5: VIKOR index and ranking for EWM, AHP, and EBWM.

S.No	Equal weight method (EWM)				Analytic hierarchy process (AHP)				Entropy-based weights method (EBWM)			
	U_i	R_i	Q_i	Rank	U_i	R_i	Q_i	Rank	U_i	R_i	Q_i	Rank
1	0.608	0.333	0.778	17	0.721	0.630	0.945	18	0.552	0.451	0.621	14
2	0.609	0.318	0.729	13	0.722	0.601	0.908	16	0.541	0.386	0.532	12
3	0.648	0.310	0.757	16	0.770	0.586	0.942	17	0.554	0.290	0.421	9
4	0.495	0.302	0.529	8	0.651	0.571	0.791	15	0.387	0.258	0.255	5
5	0.508	0.279	0.473	5	0.653	0.527	0.735	13	0.395	0.193	0.181	3
6	0.574	0.264	0.511	7	0.705	0.498	0.754	14	0.454	0.245	0.289	7
7	0.398	0.217	0.130	2	0.543	0.410	0.458	11	0.268	0.170	0.058	2
8	0.464	0.242	0.297	4	0.576	0.381	0.457	10	0.349	0.256	0.225	4
9	0.397	0.256	0.252	3	0.594	0.483	0.611	12	**0.227**	**0.149**	**0.000**	**1**
10	0.776	0.333	1.000	18	0.628	0.293	0.397	8	0.898	0.548	1.000	18
11	0.635	0.275	0.625	11	0.569	0.337	0.391	7	0.697	0.451	0.729	16
12	0.669	0.294	0.733	14	0.570	0.308	0.353	6	0.756	0.483	0.813	17
13	0.637	0.263	0.591	10	0.546	0.264	0.268	4	0.706	0.386	0.655	15
14	0.575	0.333	0.735	15	0.533	0.260	0.249	2	0.582	0.351	0.519	11
15	**0.477**	**0.177**	**0.105**	**1**	0.491	0.308	0.265	3	0.461	0.225	0.270	6
16	0.519	0.323	0.629	12	**0.317**	**0.252**	**0.000**	**1**	0.663	0.341	0.565	13
17	0.588	0.253	0.493	6	0.586	0.337	0.409	9	0.578	0.266	0.409	8
18	0.575	0.283	0.573	9	0.559	0.293	0.321	5	0.571	0.298	0.443	10

of the diversity index. This diversity index gives the quantitative measure of an individual criterion distributed among the alternatives. The concept of weight measurement is that a greater index value than a lower index value is preferable [26].

Based on EBWM, the respective weights of MRR, ROC, and CF are 0.101, 0.351, and 0.548, respectively.

Step 4. Determine the utility measure (U_i) and regret measure (R_i).

From the NDM, find the maximum value ($NDM_{\max}$) and the minimum value ($NDM_{\min}$) for both beneficial and nonbeneficial criteria. In this machining process, MRR is the beneficial criterion, whereas ROC and CF are the nonbeneficial criteria.

For beneficial criterion, the U_i and R_i terms are expressed in the following equations and represented in Table 5.

$$U_i = \sum_{i=1}^{n} W_i \frac{\left(NDM_{ij} - NDM_{\min}\right)}{\left(NDM_{\max} - NDM_{\min}\right)}, \tag{5}$$

$$R_i = \text{Max.of}\left[W_i \frac{\left(NDM_{\max} - NDM_{ij}\right)}{\left(NDM_{\max} - NDM_{\min}\right)}\right]. \tag{6}$$

For the nonbeneficial criterion, the *Ui* and *Ri* terms are expressed in the following equations:

$$U_i = \sum_{i=1}^{n} W_i \frac{\left(NDM_{\max} - NDM_{ij}\right)}{\left(NDM_{\max} - NDM_{\min}\right)}, \tag{7}$$

$$R_i = \text{Min.of}\left[W_i \left[\frac{\left(NDM_{ij} - NDM_{\min}\right)}{\left(NDM_{\max} - NDM_{\min}\right)}\right]\right]. \tag{8}$$

Step 5. Determine the value of Q_i

The value of Q_i can be computed by the following equation, where U_i is the utility measure, (U_i) max = maximum of U_i, (U_i)min = minimum of U_i.

$$Q_i = \left[\epsilon \left[\frac{\left(U_i - (U_i)_{\min}\right)}{\left((U_i)_{\max} - (U_{i\min})\right)}\right]\right] + \left[[1-\epsilon]\left[\frac{\left(R_i - (R_i)_{\min}\right)}{\left((R_i)_{\max} - (R_{i\min})\right)}\right]\right], \tag{9}$$

whereas R_i is the regret measure, (R_i) max = maximum of R_i, (R_i)min = Minimum of R_i and is introduced for weight for the strategy of maximum criteria. The value normally lies between 0 and 1 and it is now considered as 0.5.

Step 6. Ranking of alternatives

The alternatives ranking is based on the value of Q_i. The minimum value of Q_i gives the best alternative among all alternatives.

3.2. Confirmation Test. After assessing the optimal parameters from the VIKOR method based on different weights by EWM, AHP, and EBWM. A confirmation test was carried out to validate the VIKOR method outcomes. To estimate the optimum MRR, ROC, and CF (10) were used, respectively.

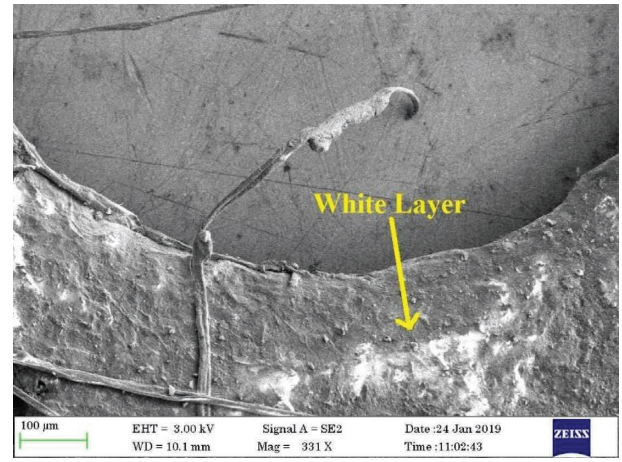

Figure 6: Process parameters effect on CF.

$$\mathfrak{R} = Q_m + \sum_{i=1}^{q} \left(Q_i - Q_m\right), \tag{10}$$

where Q_m is the overall VIKOR index mean, q represents the number of different control parameters and Q_i is the VIKOR index mean at optimal conditions.

Here, (A2, B2, C3, D1), (A2, B3, C1, D3), and (A1, B3, C3, D1) represent the optimum levels of MRR, ROC, and CF based on EW-VIKOR, AHP-VIKOR, and EBWM-VIKOR methods. The improvement in the VIKOR index is found to be 0.673, 0.945, and 0.621 from the different weight methods. Among the three different methods, AHP-VIKOR gives the maximum improvement of 0.945. Thus, the result of the confirmation obtained from the (10) reflects optimization success.

3.3. Micromachined Hole Scanning Electron Microscope (SEM) Image. Figure 6 shows the SEM image of a machined hole at TE = 40°C, MV = 10 V, DC = 90%, EC = 15 g/l trail. This image clearly depicts the formation of a white layer due to the increase in the temperature of the electrode. The heated electrode raises the local temperature of the electrolyte and lowers its viscosity, resulting in electrolyte regeneration in the machining zone.

4. Conclusion

In the present study, electrode heating is proposed for improving the performance of the EMM process. L_{18} mixed-level OA Taguchi design was adopted for conducting the experiments. In addition, the MCDM VIKOR method is used to find out the optimal process parameters of AMCs. The conclusions and results drawn from this research are given as follows:

(i) The EMM setup is altered with an electrode consisting of a heating coil, power supply, and thermostat.

(ii) The effect on MRR, ROC, and CF of process parameters such as the temperature of the electrode, MV, DC, and EC was investigated through L_{18} mixed-level OA, and the effect of heating the electrode on MRR, ROC, and CF was significant.

(iii) The optimal process parameters and their levels for maximizing MRR and minimizing ROC and CF using the VIKOR method were determined based on three distinct weight-assessing methods.

(iv) Optimal levels of EW-VIKOR are observed at A2 B2 C3 D1 (i.e., the temperature of TE = 40°C, MV = 10 V, DC = 90%, EC = 15 g/l). For AHP-VIKOR are observed at A2 B3 C1 D3 (i.e., the temperature of TE = 40°C, MV = 12 V, DC = 70%, EC = 25 g/l) and for EBWM are observed at A1 B3 C3 D1 (i.e., the temperature of TE = 30°C, MV = 12 V, DC = 90%, EC = 15 g/l).

(v) Based on the tests of confirmation results, the AHP-VIKOR provides a better improvement of 0.945 by the VIKOR index.

Nomenclature

AHP: Analytic hierarchy process
AMCs: Aluminium metal matrix composite
CF: Conicity factor
CM: Chemical machining
EBWM: Entropy-based weight method
EDM: Electrical discharge machining
EMM: Electrochemical micromachining
EWM: Equal weight method
GGBS: Ground granulated blast furnace slag
LBM: Laser beam machining
MRR: Material removal rate
MCDM: Multicriterion design making
NDM: Normalized decision matrix
OA: Orthogonal array
R_f: Radiofrequency
ROC: Radial overcut
SEM: Scanning electron microscope
TOPSIS: The technique for order of preference by similarity to an ideal solution
VIKOR: VlseKriterijumska Optimizacija I Kompromisno Resenje, i.e., multicriteria optimization and compromise solution.

Data Availability

The data used to support the results of this study are included within the article and are available from the corresponding author upon request.

Conflicts of Interest

The authors declare that there are no conflicts of interest.

References

[1] D. B. Miracle, "Metal matrix composites – from science to technological significance," *Composites Science and Technology*, vol. 65, no. 15-16, pp. 2526–2540, 2005.

[2] M. B. D. Ellis, "Joining of aluminium based metal matrix composites," *International Materials Reviews*, vol. 41, no. 2, pp. 41–58, 1996.

[3] A. K. Srivastava, A. R. Dixit, and S. Tiwari, "A review on the intensification of metal matrix composites and its nonconventional machining," *Science and Engineering of Composite Materials*, vol. 25, no. 2, pp. 213–228, 2018.

[4] V. K Jain, *Introduction to Micromachining*, Narosa Publishing House, New Delhi, 2010.

[5] V. Venkatesh, N. Swain, G. Srinivas, P. Kumar, and H. C. Barshilia, "Review on the machining characteristics and research prospects of conventional microscale machining operations," *Materials and Manufacturing Processes*, vol. 32, no. 3, pp. 235–262, 2016.

[6] R. Thanigaivelan, R. M. Arunachalam, M Kumar, and B. P. Dheeraj, "Performance of electrochemical micromachining of copper through infrared heated electrolyte," *Materials and Manufacturing Processes*, vol. 33, no. 4, pp. 383–389, 2017.

[7] M. Soundarrajan and R. Thanigaivelan, "Investigation on electrochemical micromachining (ECMM) of copper inorganic material using UV heated electrolyte," *Russian Journal of Applied Chemistry*, vol. 91, no. 11, pp. 1805–1813, 2018.

[8] P. Gründler and A. Kirbs, "The technology of hot-wire electrochemistry," *Electroanalysis*, vol. 11, no. 4, pp. 223–228, 1999.

[9] F. L Qiu, R. G Compton, B. A Coles, and F Marken, "Thermal activation of electrochemical processes in a Rf-heated channel flow cell: experiment and finite element simulation," *Journal of Electroanalytical Chemistry*, vol. 492, no. 2, pp. 150–155, 2000.

[10] G. G Wildgoose, D Giovanelli, N. S. Lawrence, and R. Compton, "High- temperature electrochemistry: a review," *Electroanalysis*, vol. 16, no. 6, pp. 421–433, 2004.

[11] F. Marken, "Chemical and electro-chemical applications of in situ microwave heating," *Annual Reports Section "C" (Physical Chemistry)*, vol. 104, pp. 124–141, 2008.

[12] Y. Long, Q. Liu, Z. Zhong, L. Xiong, and T. Shi, "Experimental study on the processes of laser-enhanced electrochemical micromachining stainless steel," *Optik - International Journal for Light and Electron Optics*, vol. 126, no. 19, pp. 1826–1829, 2015.

[13] S Maniraj and R Thanigaivelan, "Optimization of electrochemical micromachining process parameters for machining of AMCs with different % compositions of GGBS using Taguchi and TOPSIS methods," *Transactions of the Indian Institute of Metals*, vol. 72, no. 12, pp. 3057–3066, 2019.

[14] B Singaravel and T. Selvaraj, "Optimization of machining parameters in turning operation using combined TOPSIS and AHP method," *Tehnički Vjesnik - Technical Gazette*, vol. 22, pp. 1475–1481, 2015.

[15] R. Kumar, P. S Bilga, and S. Singh, "Multi objective optimization using different methods of assigning weights to energy consumption responses, surface roughness and material removal rate during rough turning operation," *Journal of Cleaner Production*, vol. 164, pp. 45–57, 2017.

[16] D. Singh and R. Shukla, "Parameter optimization of electrochemical machining process using black hole algorithm,"

IOP Conference Series: Materials Science and Engineering, vol. 282, Article ID 012006, 2017.

[17] H. Sohrabpoor, S. P. Khanghah, S. Shahraki, and R. Teimouri, "Multi-objective optimization of electrochemical machining process," *International Journal of Advanced Manufacturing Technology*, vol. 82, no. 9-12, pp. 1683–1692, 2015.

[18] R. K. Bhuyan and B. C. Routara, "Optimization the machining parameters by using VIKOR and Entropy Weight method during EDM process of Al–18% SiCp Metal matrix composite," *Decision Science Letters*, vol. 5, pp. 269–282, 2016.

[19] S. Maniraj and R Thanigaivelan, "Effect of electrode heating on performance of electrochemical micromachining," *Materials and Manufacturing Processes*, vol. 34, no. 13, pp. 1494–1501, 2019.

[20] M. K Sahu and R. K. Sahu, *Fabrication of Aluminum Matrix Composites by Stir Casting Technique and Stirring Process Parameters Optimization*Intech, 2018.

[21] Z. W. Fan and L. W. Hourng, "Electrochemical micro-drilling of deep holes by rotational cathode tools," *International Journal of Advanced Manufacturing Technology*, vol. 52, no. 5-8, pp. 555–563, 2011.

[22] P. Gründler, T. Zerihun, A Möller, and A. Kirbs, "A simple method for heating micro electrodes in-situ," *Journal of Electroanalytical Chemistry*, vol. 360, no. 1-2, pp. 309–314, 1993.

[23] G. U. Flechsig and A. Walter, "Electrically heated electrodes: practical aspects and new developments," *Electroanalysis*, vol. 24, no. 1, pp. 23–31, 2011.

[24] C. J. T. Mariapushpam, D. Ravindran, and M. D. Anand, "Machining parameters influencing in electro chemical machining on AA6061 MMC," *Materiali in tehnologije*, vol. 50, no. 6, pp. 951–960, 2016.

[25] C. S. Kalra, V. Kumar, and A. Manna, "Analysis of electrochemical behavior on micro-drilling of cast hybrid Al/(Al2O3p + SiCp + Cp)-MMC using micro-ECM process," *Proceedings of the Institution of Mechanical Engineers - Part L: Journal of Materials: Design and Applications*, vol. 232, no. 1, pp. 67–79, 2015.

[26] T. L. Saaty, "Decision making with the analytic Hierarchy process," *International Journal of Services Sciences*, vol. 1, pp. 83–98, 2008.